

Gap-state formation in two-dimensional ordered Bi layers on InAs(110)

Maria Grazia Betti, Valdis Corradini, Umberto del Pennino, Valentina De Renzi, Paolo Fantini, and Carlo Mariani
*Istituto Nazionale per la Fisica della Materia, Dipartimento di Fisica, Università di Modena, via G. Campi 213/A,
 I-41100 Modena, Italy*

(Received 19 February 1998)

The spectral density at the Fermi energy and the formation of adlayer-induced electronic states is studied by means of high energy resolution ultraviolet photoemission spectroscopy. A highly ordered (1×1)-Bi monolayer deposited on InAs(110) induces a well-resolved, occupied electronic state in the InAs surface gap, attributed to *p*-like dangling bonds at the Bi atomic chains. Appropriate annealing of a Bi multilayer produces a (1×2)-symmetry stable phase. Evolution of the spectral density close to the Fermi edge brings to light the metallicity of the (1×2)-Bi layer induced by Bi—Bi bonding in the atomic chains. [S0163-1829(98)50432-8]

The (110) surfaces of III-V compound semiconductors constitute viable substrates for investigating the electronic properties of group-V two-dimensional (2D) ordered layers, thanks to their widely recognized unreactive and epitaxial interfaces.^{1–26} Antimony and bismuth grow on GaAs(110) with a (1×1)-symmetry epitaxial continued-layer structure (ECLS), with the group-V atoms continuing the underlying bulklike structure of the III-V substrate. Conversely, Bi can build up not only (1×1) structure on narrow-gap III-V's, but also a (1×2)-symmetry geometry as the stable, thermally achievable phase. These two-dimensional ordered layers give rise to different electronic responses depending on their actual atomic geometry.

The (1×1)-symmetry ECLS Bi layers are generally semi-conducting, as has been experimentally and theoretically demonstrated,^{6,11,27–30} while the (1×2)-Bi layers present a low spectral density at the Fermi level, according to the available experimental data.²³ However, the lack of exhaustive experimental and theoretical information on the (1×2)-Bi layer on InAs(110), requires a careful experimental study of the evolution of Bi-induced electronic states, following the formation of the (1×2) superstructure.

In this communication we present a high energy resolution and high-luminosity ultraviolet photoemission spectroscopy (UPS) measurement of the valence-band and energy-gap region of the Bi/InAs(110) system. High energy resolution and luminosity are essential tools for bringing to light 2D insulator-to-metal transition in narrow-gap interfaces. We particularly investigate the 2D ordered (1×1)-Bi monolayer as-deposited at room temperature (RT) and the stable (1×2)-Bi reconstructed phase, achieved via thermal annealing. A well-resolved Bi-derived occupied state in the InAs surface energy gap is identified in the (1×1) semiconducting monolayer, while a finite spectral density is measured at the Fermi level when the (1×2)-Bi phase is formed. Its persistence at low temperature is an indication of a metallic state.

Experiments were performed at the surface physics laboratory LOTUS, Dipartimento di Fisica, Università di Modena. A high-resolution hemispherical electron analyzer Scienta SES-200 was contained in an ultrahigh vacuum (UHV) chamber, equipped with a high-intensity UV He discharge source and low-energy electron-diffraction (LEED),

the UHV chamber was connected to a preparation chamber containing all ancillary facilities for crystal preparation and Bi deposition. Base pressure in the chambers was in the low 10^{-10} mbar (10^{-8} Pa) range. The InAs(110) surface was obtained by cleaving an *n*-type doped single crystal ($n \sim 2 \times 10^{18}$ cm⁻³) with the single wedge technique. Bismuth was evaporated by a resistively heated quartz crucible, deposited on the substrate at room temperature, with an evaporation rate of about 1 Å/min. The overlayer thickness was determined with an oscillating quartz microbalance and checked with the In-4*d* and Bi-5*d* core level intensity behavior. One monolayer (ML) is defined as a Bi atomic density equivalent to the surface atomic density of InAs(110) (7.75×10^{14} cm⁻²). The growth morphology was followed by Auger electron spectroscopy and was characterized by A Stranski-Krastanov behavior, with the completion of the first (1×1) ordered ML followed by 3D island formation and eventually by polycrystalline Bi arrangement.^{30–32} The stable (1×2)-symmetry phase was obtained by annealing a 20-ML thick Bi layer in several steps for 20 min at progressively higher temperatures. The (1×2) phase was stable between 250 and 310 °C. The (1×2) layer was also prepared by annealing a few ML thick layer at 290 °C for about 20 min. Symmetry and order were checked via LEED observations. The electron analyzer was set at a 10 eV pass energy, with an instrumental energy resolution of 15 meV, as determined on the Fermi level of freshly evaporated Au in good electrical contact with the InAs crystal. Valence-band spectra were taken with HeI photons (21.218 eV) impinging onto the surface with 18° incidence angle and photoemitted electrons were analyzed at normal emission with an angle integration of $\sim \pm 6^\circ$.

Photoemission energy distribution curves (EDC's) close to valence-band maximum (VBM), at different Bi coverage stages, are shown in Fig. 1 in a perspective view, to enlighten the evolution of Bi-induced states in the narrow band-gap region and the spectral density evolution close to the Fermi energy. Clean InAs(110) presents the VBM at about 0.4 eV below the Fermi energy, in agreement with the expected position determined by the high *n*-type doping level.³³ The main effect of Bi deposition is the appearance of an occupied surface state at 16.91 eV kinetic energy (KE) [0.39 eV binding energy (BE)] developing at about 1 ML

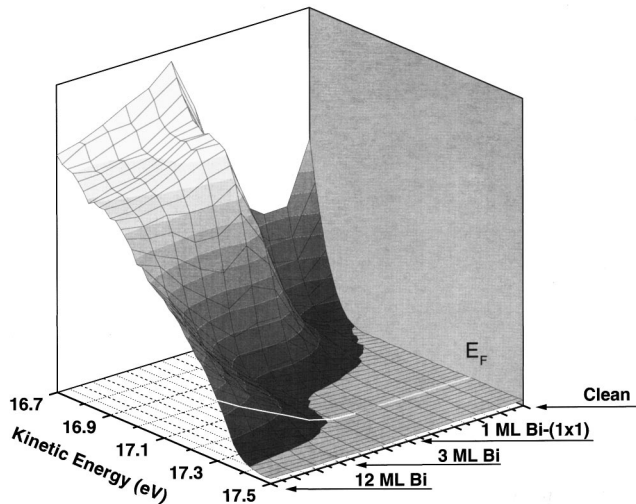


FIG. 1. Perspective view of high-resolution ultraviolet (He_I photons, 21.218 eV) photoemission spectra of the Bi/InAs(110) interface as a function of coverage, in the energy-gap region. Intensity of energy distribution curves (EDC's) is displayed in the vertical axes. Successive spectra belonging to progressive Bi deposition steps are stacked along one of the horizontal axes, while the other horizontal axes represent the kinetic energy of the photoelectrons. Notice the formation and evolution of a Bi-induced occupied state within the InAs surface gap around the (1x1) monolayer coverage.

coverage, corresponding to the ordered (1x1)-Bi phase. At this coverage the 2D system is still semiconducting, in agreement with previous angular resolved photoemission studies,^{30,31} with the VBM lying less than 0.1 eV below the Fermi level (E_F). This suggests a surface gap lower than that of the bare InAs(110) surface. Upon increasing coverage the interface further evolves with a redistribution of the spectral density from the Bi-induced state towards the Fermi energy, eventually closing the gap and becoming metallic above 2 ML Bi coverage (notice the finite density of states at E_F at 12 ML Bi).

The spectral intensity at E_F and at the Bi-induced state (16.9 eV KE) is plotted in Fig. 2, as a function of Bi coverage. This plot shows the spectral redistribution of electronic states: the Bi-induced occupied state reaches a maximum at about 1 ML coverage, while further Bi deposition moves electron density towards E_F ; we argue that the coalescence of Bi clusters determines the interface metallization.

However, we notice that the (1x1) layer is not the stable phase for the annealed Bi/InAs(110) interface. Thermal annealing of a few ML thick Bi layer causes desorption of bismuth in excess of one monolayer, producing a well-ordered (1x2)-symmetry phase, corresponding to a coverage of about 1 ML.^{8,26} Photoemission EDC's in the energy-gap region as a function of annealing temperature from RT to 360 °C, starting from a 20-ML-thick Bi layer on InAs(110), are shown in Fig. 3 in a perspective view. Annealing produces desorption of Bi in excess of about 1 ML until the (1x2) phase is formed. It is stable from 250 to about 310 °C and is characterized by a stable and definite electronic structure. A clear redistribution of the spectral density close to the top of the valence band (VB) takes place upon increasing temperature, with the formation of a low density of states at the Fermi level. The quasi-free-electronlike character of elec-

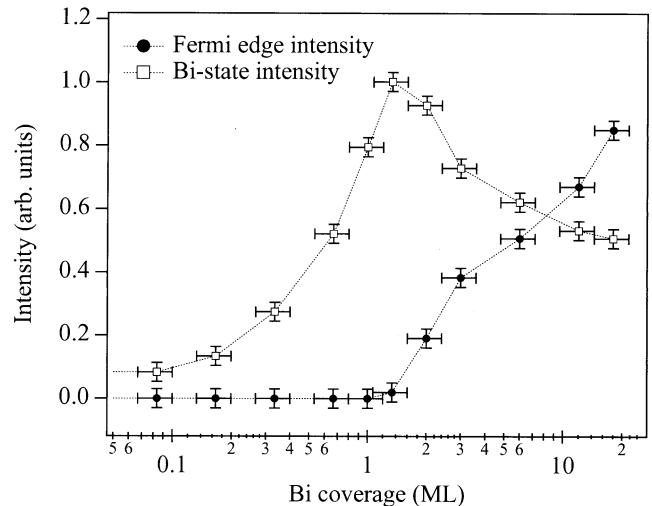


FIG. 2. Photoemission spectral intensity at E_F and at the Bi-induced state (16.9 eV KE) as a function of the Bi coverage, for the Bi/InAs(110) interface grown at RT.

trons at E_F has been checked by following the temperature dependence down to 160 K. Further annealing eventually produces complete desorption of bismuth, leaving the bare InAs(110) surface and recovering the valence band of the clean surface.

A selected set of photoemission results [(1x1)-Bi, (1x2)-Bi, and clean InAs(110)] in a wider VB energy range, is collected in Fig. 4. The clean surface presents a huge peak at 1.00 eV BE, due to the highest-occupied As dangling and back-bond surface states (A4 and A5, following the notation of Ref. 24). The (1x1)-Bi phase presents a surface state at 0.39 eV BE, a main peak at 1.04 eV, and a shoulder at 0.68

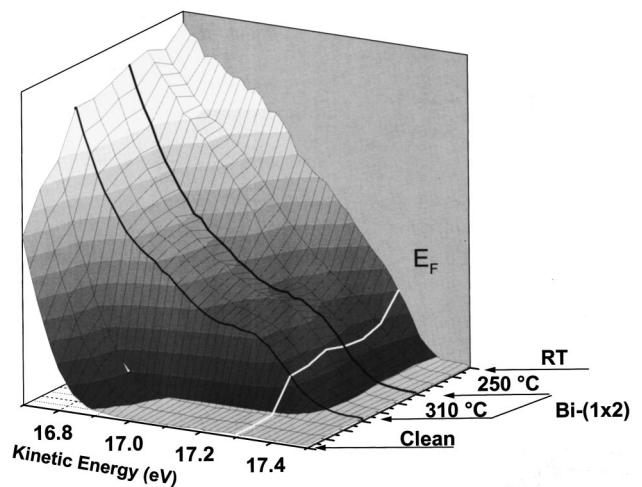


FIG. 3. Perspective view of high-resolution ultraviolet (He_I photons, 21.218 eV) photoemission spectra of the Bi/InAs(110) interface as a function of annealing temperature, in the energy-gap region. Intensity of energy distribution curves is displayed in the vertical axes. Successive spectra belonging to progressive annealing steps (from RT to 360 °C) are stacked along one of the horizontal axes, while the other horizontal axes represent the kinetic energy of the photoelectrons. Notice the evolution from the bulklike Bi semimetallic VB to the semimetallic stable (1x2)-Bi phase and eventual recovering of the gap after complete Bi desorption.

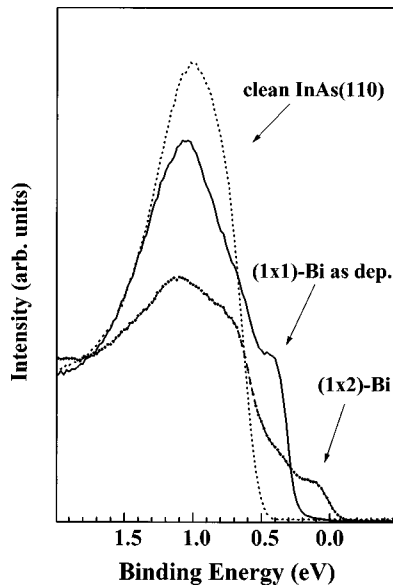


FIG. 4. High-resolution ultraviolet (He_I photons, 21.218 eV) photoemission spectra in the topmost valence-band region for the (1×1) -Bi/InAs(110) and (1×2) -Bi/InAs(110) phase. The clean InAs(110) surface data are shown for comparison.

eV, as determined by the numerical second derivative of the data. The VB shape for the (1×2) phase presents two structures at 1.13 and 0.68 eV BE, resembling those shown in the (1×1) phase, while the (1×1) -0.39 eV feature is almost suppressed, leaving a small shoulder at 0.33 eV, with a spectral density emerging at the Fermi level.

We can consider the ECLS geometry a good structural model for the (1×1) phase.²⁴ Bi grows with a shifted-ECLS geometry on GaAs(110) but is not commensurate.^{7,15,18} A better surface atomic matching between the Bi covalent radius and substrate lattice parameter can be established with a larger III-V (110) surface unit cell, like InAs(110). Recent *ab initio* pseudopotential energy-band calculations within the local-density approximation,²⁴ obtaining the ECLS as the equilibrium structure for the (1×1) -Bi phase at RT, identify the highest-occupied state of Bi (S_8) as that due to the Bi dangling bonds mainly with p -symmetry character. Thus, we

can reasonably attribute the 0.39 eV BE Bi-induced surface state to bismuth dangling bonds of the topmost atomic chains.

The actual atomic geometry of the stable (1×2) phase is not yet available. However, grazing incidence x-ray diffraction (GIXD) data on the (1×2) -Bi/GaSb(110) system²⁵ and a preliminary evaluation of very recent GIXD experiments on the (1×2) -Bi/InAs(110) system,²⁶ suggest a structural model in which the Bi chains are distorted and every second zigzag chain in the uppermost substrate layer is missing. The Bi dangling bond states are strongly influenced by the missing row superstructure. Therefore, we can infer that distortion of the Bi chains produces modification of the Bi-induced surface states in the gap region. In fact, it is well established that the topmost occupied and lowest unoccupied surface states in the ECLS geometry are extremely sensitive to the buckling of the topmost chain atoms.⁵ In particular, S_8 and S_9 ,²⁴ which correspond to dangling-bond (topmost occupied) and antibonding (lowest unoccupied) Bi chain states, respectively, in the (1×1) ECLS phase, shift with respect to the Fermi level, owing to the strong distortion experienced by the Bi chains in the formation of the (1×2) -symmetry phase. This can produce a crossing of the Fermi level and the metallic behavior of the stable (1×2) -Bi layer.

In conclusion, the formation of adlayer-induced gap states and a semiconductor-to-semimetal transition in 2D ordered Bi monolayers prepared on InAs(110), has been studied using high-resolution and high-luminosity ultraviolet photoelectron spectroscopy. Formation and evolution of bismuth-induced surface states has been followed on the Bi/InAs(110) interface as a function of coverage, indicating a dangling-bond-derived state at 0.39 eV binding energy in the monolayer coverage regime, when the semiconducting (1×1) -symmetry phase is formed. Annealing at $\sim 290^\circ\text{C}$ produces a (1×2) -symmetry Bi layer as the stable phase, presenting a definite metallic behavior. The gap states and the transition to a metallic response can be ascribed to the modification of the electronic states due to Bi bonded in atomic chains, when the chain geometric structure is deeply distorted due to the formation of the (1×2) -symmetry phase.

This work was financed under the Advanced Research Project LOTUS, of INFN. We also acknowledge partial support from the Ministero per l'Università e per la Ricerca Scientifica e Tecnologica (MURST).

¹J. Carelli and A. Kahn, *Surf. Sci.* **116**, 380 (1982).

²C. B. Duke, A. Paton, W. K. Ford, A. Kahn, and J. Carelli, *Phys. Rev. B* **26**, 803 (1982).

³C. A. Swarts, W. A. Goddard, and T. C. McGill, *J. Vac. Sci. Technol.* **17**, 982 (1982).

⁴P. Skeath, C. Y. Su, W. A. Harrison, I. Lindau, and W. E. Spicer, *Phys. Rev. B* **27**, 6246 (1983).

⁵C. Mailhot, C. B. Duke, and D. J. Chadi, *Phys. Rev. B* **31**, 2213 (1985).

⁶J. J. Joyce, J. Anderson, M. M. Nelson, and G. J. Lapeyre, *Phys. Rev. B* **40**, 10 412 (1989).

⁷A. B. McLean and F. J. Himpsel, *Phys. Rev. B* **40**, 8425 (1989).

⁸W. K. Ford, T. Guo, S. L. Lantz, K. Wan, S.-L. Chang, C. B. Duke, and D. L. Lessor, *J. Vac. Sci. Technol. B* **8**, 940 (1990).

⁹W. K. Ford, T. Guo, D. L. Lessor, and C. B. Duke, *Phys. Rev. B* **42**, 8952 (1990).

¹⁰Maria Grazia Betti, M. Pedio, U. del Pennino, and Carlo Mariani, *Phys. Rev. B* **43**, 14 317 (1991).

¹¹Maria Grazia Betti, M. Pedio, U. del Pennino, and Carlo Mariani, *Phys. Rev. B* **45**, 14 057 (1992).

¹²G. P. Srivastava, *Phys. Rev. B* **46**, 7300 (1992); **47**, 16 616 (1993).

¹³G. P. Srivastava, *J. Phys.: Condens. Matter* **5**, 4695 (1993).

¹⁴T. Kendelewicz, J. C. Woicik, A. Herrera-Gomez, K. E. Miyano, P. L. Cowan, B. A. Karlin, P. Pianetta, and W. E. Spicer, *J. Vac. Sci. Technol. A* **11**, 2351 (1993).

¹⁵A. Herrera-Gomez, T. Kendelewicz, J. C. Woicik, K. E. Miyano, P. Pianetta, S. Southworth, P. L. Cowan, B. A. Karlin, and W. E.

- Spicer, J. Vac. Sci. Technol. A **11**, 2354 (1993).
- ¹⁶F. Bechstedt, W. G. Schmidt, and B. Wenzien, Europhys. Lett. **25**, 357 (1994).
- ¹⁷W. G. Schmidt, B. Wenzien and F. Bechstedt, Phys. Rev. B **49**, 4731 (1994).
- ¹⁸A. Ruocco, N. Jedrecy, R. Pinchaux, M. Sauvage-Simkin, A. Waldhauer, Maria Grazia Betti, and Carlo Mariani, Phys. Rev. B **50**, 8004 (1994).
- ¹⁹Maria Grazia Betti, Carlo Mariani, N. Jedrecy, R. Pinchaux, A. Ruocco, and M. Sauvage-Simkin, Phys. Rev. B **50**, 14 336 (1994).
- ²⁰Luca Gavioli, Maria Grazia Betti, Paolo Casarini, and Carlo Mariani, Phys. Rev. B **49**, 2911 (1994).
- ²¹L. Gavioli, M. G. Betti, P. Casarini, and C. Mariani, Phys. Rev. B **51**, 16 822 (1995).
- ²²M. G. Betti, D. Berselli, C. Mariani, J. Electron Spectrosc. Relat. Phenom. **76**, 465 (1995).
- ²³D. Berselli, M. G. Betti, L. Gavioli, and C. Mariani, Surf. Sci. **331-333**, 496 (1995).
- ²⁴A. Umerski and G. P. Srivastava, Phys. Rev. B **51**, 2334 (1995).
- ²⁵T. van Gemmeren, L. Lottermoser, G. Falkenberg, L. Seehofer, R. L. Johnson, L. Gavioli, C. Mariani, R. Feidenhans'l, E. Landemark, D. Smilgies, and M. Nielsen, Phys. Rev. B **57**, 3749 (1998).
- ²⁶M. Sanvage *et al.* (unpublished).
- ²⁷A. Tulke, M. Mattern-Klosson, and H. Lüth, Solid State Commun. **59**, 303 (1986); A. Tulke and H. Lüth, Surf. Sci. **178**, 131 (1986).
- ²⁸P. Mårtensson, G. V. Hansson, M. Lähdeniemi, R. O. Magnusson, S. Wiklund, and J. M. Nicholls, Phys. Rev. B **33**, 7399 (1986).
- ²⁹G. Annovi, Maria Grazia Betti, U. del Pennino, and Carlo Mariani, Phys. Rev. B **41**, 11 978 (1990).
- ³⁰D. N. McIlroy, D. Heskett, A. B. McLean, R. Ludeke, H. Munekata, and N. J. DiNardo, J. Vac. Sci. Technol. B **11**, 1486 (1993); Phys. Rev. B **48**, 11 897 (1993).
- ³¹D. Heskett, D. McIlroy, D. M. Swanston, A. B. McLean, N. J. DiNardo, H. Munekata, and R. Ludeke, J. Vac. Sci. Technol. B **10**, 1949 (1992).
- ³²M. G. Betti *et al.* (unpublished).
- ³³Due to the high doping, the Fermi level is strongly pinned, and we estimate it to lie about 70 meV within the conduction band minimum [S. M. Sze, *Physics of Semiconductor Devices* (Wiley, New York, 1981)].